Neuroendocrinology Letters Volume 44 No. 3 2023
ISSN: 0172-780X; ISSN-L: 0172-780X; Electronic/Online ISSN: 2354-4716
Web of Knowledge / Web of Science: Neuroendocrinol Lett
Pub Med / Medline: Neuro Endocrinol Lett

ORIGINAL ARTICLE

Impact of prepubertal obesity induced by high-fat diet during lactation and post-weaning on puberty initiation and neuroendocrine function in a female mouse model.

Mengmeng Shi[1], Shi Ren[2], Yue Zhang[1], Qinling Yang[1], Lingling Zhai[1]

1 Department of Maternal, Child and Adolescent Health, School of Public Health, China Medical University, Shenyang,110122, China.
2 Department of Nutrition and Food Hygiene, Liaoning Center for Disease Prevention Control, Shenyang, 110001, China.

Correspondence to: Lingling Zhai
Department of Maternal, Child and Adolescent Health, School of Public Health, China Medical University, No.77 Puhe Road, Shenyang North New Area, Shenyang,Liaoning, 110122, China
TEL: :+86 18900910676, E-MAIL: llzhai@cmu.edu.cn

Submitted: 2022-11-24 Accepted: 2023-05-11 Published online: 2023-05-11

Key words: **High fat diet; Puberty; prepubertal obesity; Endocrine; miRNAs**

Neuroendocrinol Lett 2023; **44**(3):140–151 **PMID:** 37392441 NEL440323A08

Abstract

PURPOSE: To explore the effects of prepubertal obesity induced by high-fat diet during lactation and post-weaning on puberty onset and the neuroendocrine changes before puberty onset in a female mouse model, which may explain obesity in children starting early puberty.

METHODS: A total of 72 female mice were assigned to the high fat diet group (HFD) and the control diet group (CONT) during lactation and post-weaning. The bodily indexes; pathological changes; and protein and gene expression levels in the hypothalamus were examined on postnatal days (P) 15, 28, and 45, respectively.

RESULTS: The average vaginal opening time in HFD mice occurred significantly earlier than that in CONT mice ($p < 0.05$). On P15, no significant difference in the MKRN3, kisspeptin, GPR54 and GnRH level between HFD and CONT mice was noted ($p > 0.05$). Whereas on P28 and 45, compared to CONT mice, GnRH expression in HFD mice was significantly increased ($p < 0.05$); kisspeptin and GPR54 expression in HFD mice was also significantly increased ($p < 0.05$); but the MKRN3 level in HFD mice was significantly lower than that in CONT mice ($p < 0.05$). On P15, 28, and 45, compared with CONT mice, miR-30b expression in HFD mice increased ($p < 0.05$). Compared to P15, miR-30b, KiSS-1, GPR54 and GnRH mRNA level increased significantly, however MKRN3 decreased significantly in HFD mice on P28 and 45 ($p < 0.01$).

CONCLUSIONS: Prepubertal obesity induced by high-fat diet during lactation and post-weaning may advance the time of pubertal initiation in female mice. The increased expression of miR-30b, kisspeptin, GPR54 and GnRH, decreased the expression of MKRN3 may explain the early onset of puberty in obese female mice.

Abbreviations:
E2 - estradiol
GnRH - gonadotropin-releasing hormone
GPR54 - protein coupled receptor 54
HPG - hypothalamus–pituitary–gonadal
LH - luteinizing hormone
miRNAs - Micro-ribonucleic acids
MKRN3 - makorin ring finger protein 3

INTRODUCTION

Puberty is a key event of sexual maturity that culminates in reproductive ability (Wood *et al.* 2019). In the past half century, puberty initiation has been reported to commence at an earlier age in females (Biro *et al.* 2018; Eckert-Lind *et al.* 2020; Krieger *et al.* 2015). Studies have reported that early type 2 diabetes, cardiovascular disease, and adverse psychological and behavioral factors are closely associated with early-onset puberty (Biro *et al.* 2018; Cheng *et al.* 2020; Vogelezang *et al.* 2020). Furthermore, early-onset puberty is a risk factor for impaired fertility and breast cancer development (Collaborative Group on Hormonal Factors in Breast Cancer, 2012; Jacobsen *et al.* 2009). Therefore, more attention should be paid to early-onset puberty and its effects later in life.

Pubertal development can be influenced by environmental and genetic factors (Huang & Roth, 2021; Zhou *et al.* 2022). Some studies have reported that adverse environmental factors early in life can affect puberty initiation (Greenspan & Lee, 2018; Colich *et al.* 2020; Livadas & Chrousos, 2019). In particular, several investigators have examined the impact of nutrition early in life (pregnancy, lactation, and childhood) (Ribaroff *et al.* 2017; Connor *et al.* 2012), while we have researched the effects of prepubertal obesity on pubertal development and reported that prepubertal obesity may affect puberty onset (Huang *et al.* 2020). Furthermore, according to the World Health Organization, in 2016, more than 124 million children and adolescents, with a female proportion of 6%, were obese (World Health Organization, 2022). In China, the rates of childhood and adolescent obesity continue to increase annually. From 1997 to 2011, the prevalence of overweight and obesity increased from 4.6% to 10.4% in young females (Wang *et al.* 2017). Therefore, it is important to explore the effects of prepubertal obesity on pubertal development because of the high incidence of obesity in this population worldwide (Xu *et al.* 2021).

In general, the results of studies on the effects of prepubertal obesity on pubertal development in young females are consistent, and they indicate that pubertal development begins earlier in obese young females (Huang *et al.* 2020). For example, Wu *et al.* (2012) demonstrated that obesity can lead to the earlier opening of the vaginal orifice and the thickening of the follicular intima in female rats. However, the mechanism of early-onset puberty caused by prepubertal obesity in females is unclear.

In our earlier study, we demonstrated that increased estradiol (E2) levels could induce early-onset puberty in obese young females (Zhai *et al.* 2015). The changes in sex hormone levels during puberty are mainly regulated by the hypothalamus–pituitary–gonadal (HPG) axis, and the activation of the HPG axis is required for pubertal development, with changes in the secretion of gonadotropin-releasing hormone (GnRH) playing

Tab. 1. Primers for real-time PCR

Gene		Base sequence
GnRH	Forward	5′-GTACTCAACCTACCAACGGAAGCTC-3′
	Reverse	5′-CGCAACCCATAGGACCAGTG-3′
KiSS-1	Forward	5′-CCCAGAATGATCTCAATGGCTTCT-3′
	Reverse	5′-CTCTCTGCATACCGCGATTCCT-3′
GPR54	Forward	5′GCAGCCCATGGTTGAAGCTAA-3′
	Reverse	5′-AGCTATGCCCGGATGACAGAAG-3′
MKRN3	Forward	5′-AGGAGGAAGAGGAGAAGGAGAA-3′
	Reverse	5′CCAGGCGAAGCACAGAATG-3′
miR-30b	RT Primer	5′-GTCGTATCCAGTGCGTGTCGTGGAGTCGGCAATTGCACTGGATACGACAGCTGAC-3′
	Forward	5′-GGTGTAAACATCCTACACT-3′
U6	Reverse	5′-CAGTGCGTGTCGTGGAGT-3′
	Forward	5′-CTCGCTTCGGCAGCACAT-3′
	Reverse	5′-AAATATGGAACGCTTCACG-3′
β-actin	Forward	5′-CATCCGTAAAGACCTCTATGCCAAC-3′
	Reverse	5′-ATGGAGCCACCGATCCACA-3′

GnRH: gonadotropin-releasing hormone; GPR54: G protein-coupled receptor 54; MKRN3: makorin ring finger protein 3; miR-30b: microRNA-30b.

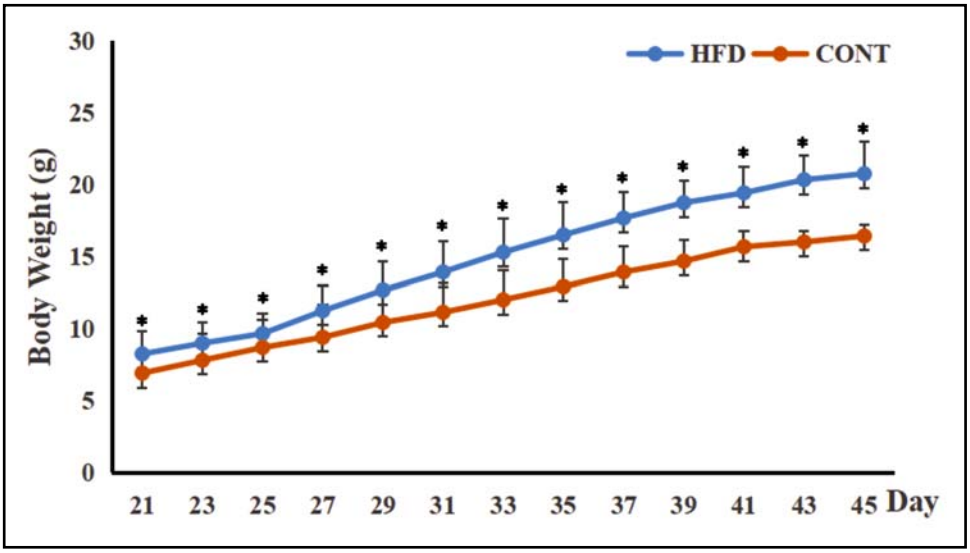

Fig. 1. Comparison of body weight between obese and control mice from postnatal day 21 to 45. The body weight changes between obese and control mice from postnatal day 21 to 45. Data are presented as mean±SD, n = 12. *$P < 0.05$ as compared to the CONT. HFD: high-fat diet; CONT: control; SD: standard deviation.

key roles in these events (Herbison, 2016; Terasawa & Fernandez, 2001). Although the secretion of GnRH by the hypothalamus and its mechanism of action are complex, we investigate early-onset puberty caused by prepubertal obesity in females by studying the GnRH pathway.

Micro-ribonucleic acids (microRNAs, miRNAs) are non-coding single-stranded RNA molecules that are comprised of approximately 22 nucleotides (Agbu & Carthew, 2021). MiRNAs play important roles in pubertal development. For example, Heras *et al.* (2019) reported that miR-30 can regulate the onset of puberty. Although it is unclear whether GnRH is involved in this process, miR-30 can affect pubertal development by regulating the makorin ring finger protein 3 (MKRN3)/kisspeptin pathway (Heras *et al.* 2019). MKRN3 is an indispensable component of the regulatory network that controls the onset of puberty, and it has been reported that miR-30 has an inhibitory effect on MKRN3 expression (Heras *et al.* 2019). In another study, MKRN3 expression was elevated during prepuberty, at which time MKRN3 inhibited GnRH secretion, which is quiescent at this stage of development (Abreu & Kaiser, 2016). Upon puberty initiation, MKRN3 expression decreases, GnRH secretion increases, and pubertal development initiates (Abreu & Kaiser, 2016). On the other hand, kisspeptin is a neuropeptide encoded by the KiSS-1 gene that binds to G protein coupled receptor 54 (GPR54) and directly acts on GnRH-expressing neurons to stimulate GnRH release and regulate the HPG axis (Harter *et al.* 2018). A previous study has reported that MKRN3 can affect GnRH secretion by inhibiting kisspeptin activity (Abreu *et al.* 2020). Furthermore, miR-30 expression was increased in obese mice (Sangiao-Alvarellos *et al.* 2014), which prompted us to hypothesize that elevated miR-30 expression can inhibit MKRN3 expression, promote kisspeptin and GnRH expression, and initiate early-onset puberty in obese female mice.

Thus, this study explores the effects of prepubertal obesity induced by high-fat diet during lactation and post-weaning on puberty onset and the neuroendocrine changes before puberty onset in a female mouse model, which may explain obesity in children starting early puberty and involve changes in the expression of miR-30b, MKRN, kisspeptin, GPR54, and GnRH during pubertal development.

MATERIALS AND METHODS

Animals

All experimental procedures were conducted in accordance with the Institutional Guidelines for the Care and Use of Laboratory Animals at China Medical University (Shenyang, China) (CMU2019186) and the National Institutes of Health Guide for Care and Use of Laboratory Animals (publication no. 85-23, revised 1985) under experimental protocol no. SYXK (Liao) 2018-0008.

Dams: A total of 36 C57BL-6J mice (12 males and 24 females) were obtained from Beijing HFK Bioscience Co., Ltd. (Beijing, China). Male and female C57BL-6J mice (10-weeks-of-age) were housed in a single room with 12 h:12 h light–dark cycles and a constant temperature of 25°C, and all mice were provided standard chow and water *ad libitum*. According to the study of Connor *et al.* on the following morning, mating was confirmed by the presence of sperm in vaginal smears, and the pregnant mice were housed individually (Connor *et al.* 2012). All pregnant mice were provided standard chow and water *ad libitum* until postnatal day (P) 0. Thereafter, 24 pregnant mice were randomly assigned to a group and given one of two diets (normal diet [CONT] or high-fat diet [HFD]) during lactation, with 12 pregnant mice given the CONT diet and 12 pregnant mice given the HFD. Pups were weighed and sexed at birth. To guarantee that each pup had access to nutrition until weaning, pups were adjusted to six per litter

Tab. 2. Changes of body weight, body fat, reproductive organ weight, sex hormones of female mice at PND 45 ($\bar{x}$±SD, n=12)

group	Body weight (g)	Body fat (g)	Body fat percent (%)	Ovary weight(g)	Ovary coefficient (g/100g)	Uterus weight(g)	Uterus coefficient (g/100g)	Estradiol[a] (pg/mL)	LH[a] (mIU/mL)
HFD	19.50±2.07**	1.46±0.50**	7.30±2.32*	0.01±0.001**	0.05±0.01**	0.09±0.04**	0.43±0.18*	25.09±3.98*	4.27±0.49*
CONT	16.17±1.03	0.95±0.15	5.75±0.86	0.006±0.002	0.04±0.01	0.04±0.02	0.26±0.14	20.42±1.87	3.49±0.58

Ovary coefficient=Ovary weight/Body weight×100; Uterus coefficient=Uterus weight/Body weight×100; *P < 0.05, **P < 0.01 as compared to the CONT. a: n=8.
PND 45: postnatal day 45; LH: Luteinizing hormone; HFD: high-fat diet; CONT: control; SD: standard deviation.

(3 males and 3 females) on P2, and the remaining pups were killed by decapitation. Three females from each litter were used in this experiment, while three males from each litter were used in another experiment.

Offspring: From weaning (P22), the pups were weighed every 2 days until P45. At weaning, the female offspring were given one of two diets (CONT diet or HFD) depending on the diet the dams were given, that is, the offspring of dams fed a CONT diet also received a CONT diet with water and the offspring of dams fed a HFD also received a HFD with water until the end of the experiment. This experiment yielded two groups of post-weaned offspring, namely, CONT-cont and HFD-hfd. A total 72 (36 CONT-cont and 36 HFD-hfd) female offspring were used in the three experiments (n = 24 per experiment).

Diets

The HFD (cat. no. TP23300) was procured from Trophic Animal Feed High-Tech Co., Ltd. (Beijing, China). In the HFD, 60% of the total calories were from fat, 19% were from protein, and 21% were from carbohydrates [5 kcal/g]. In the CONT diet, 12.95% of the total calories were from fat, 24.02% were from protein, and 12.95% were from carbohydrates [3.44 kcal/g].

Definition of obesity

Obesity was evident when the body weights of HFD mice were significantly higher than those of CONT mice on P21 (weaning) (Yang *et al.* 2014; Xu *et al.* 2019).

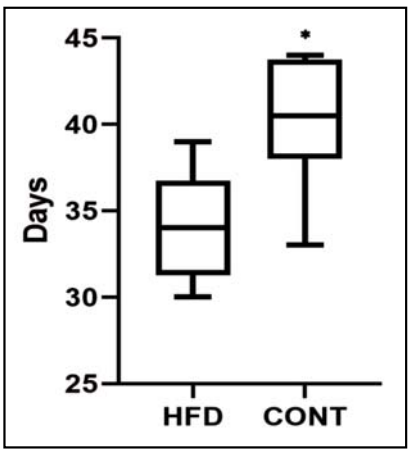

Fig. 2. Comparison of the average vaginal opening times between obese and control mice. Data are presented as mean±SD, n = 12. *P < 0.05, as compared to the CONT. HFD: high-fat diet; CONT: control; SD: standard deviation.

Experimental design

Forty-five-day experiment (puberty completion)

Twenty-four female offspring (n = 1 per litter) were divided into two groups: the HFD group (dam HF + pup hfd, n = 12) and the CONT group (dam CONT + pup cont, n = 12). The offspring were fed until P45 (puberty completion). The vaginal opening time was determined (the vaginal opening time is an indicator of puberty initiation in female mice), and the body composition and body weight of the mice were measured with a body composition analyzer (Minispec LF-50, Bruker, Germany) on P44. On P45, and after fasting for 24 h, the mice were anesthetized with diethyl ether, and blood was collected. The hypothalami were removed immediately, followed by the uteri and ovaries, which were weighed. Four hypothalami and three ovaries were fixed in 4% paraformaldehyde for immunohistochemical analysis or hematoxylin–eosin staining. Another three ovaries were fixed in 2.5% glutaraldehyde for morphological preservation and transmission electron microscopy. The remaining tissues were frozen in liquid nitrogen and stored at -80°C for western blotting (three hypothalami) and quantitative polymerase chain reaction (qPCR) (six hypothalami).

Twenty-eight-day experiment (puberty initiation)

Twenty-four female offspring were used for this experiment. The offspring were fed until P28 (puberty initiation). On P28, and after fasting for 24 h, the mice were anesthetized with diethyl ether, and blood was collected. The hypothalami were removed immediately, followed by the uteri and ovaries, which were weighed. The remaining tissues were frozen in liquid nitrogen and stored at -80°C for western blotting (four hypothalami) and qPCR (six hypothalami).

Fifteen-day experiment (prepuberty period)

Twenty-four female offspring were used for this experiment. The offspring were fed until P15 (prepuberty period). On P15, and after fasting for 24 h, the mice were anesthetized with diethyl ether, and blood was collected. The hypothalami were removed immediately, frozen in liquid nitrogen, and stored at -80°C for western blotting (four hypothalami) and qPCR (six hypothalami).

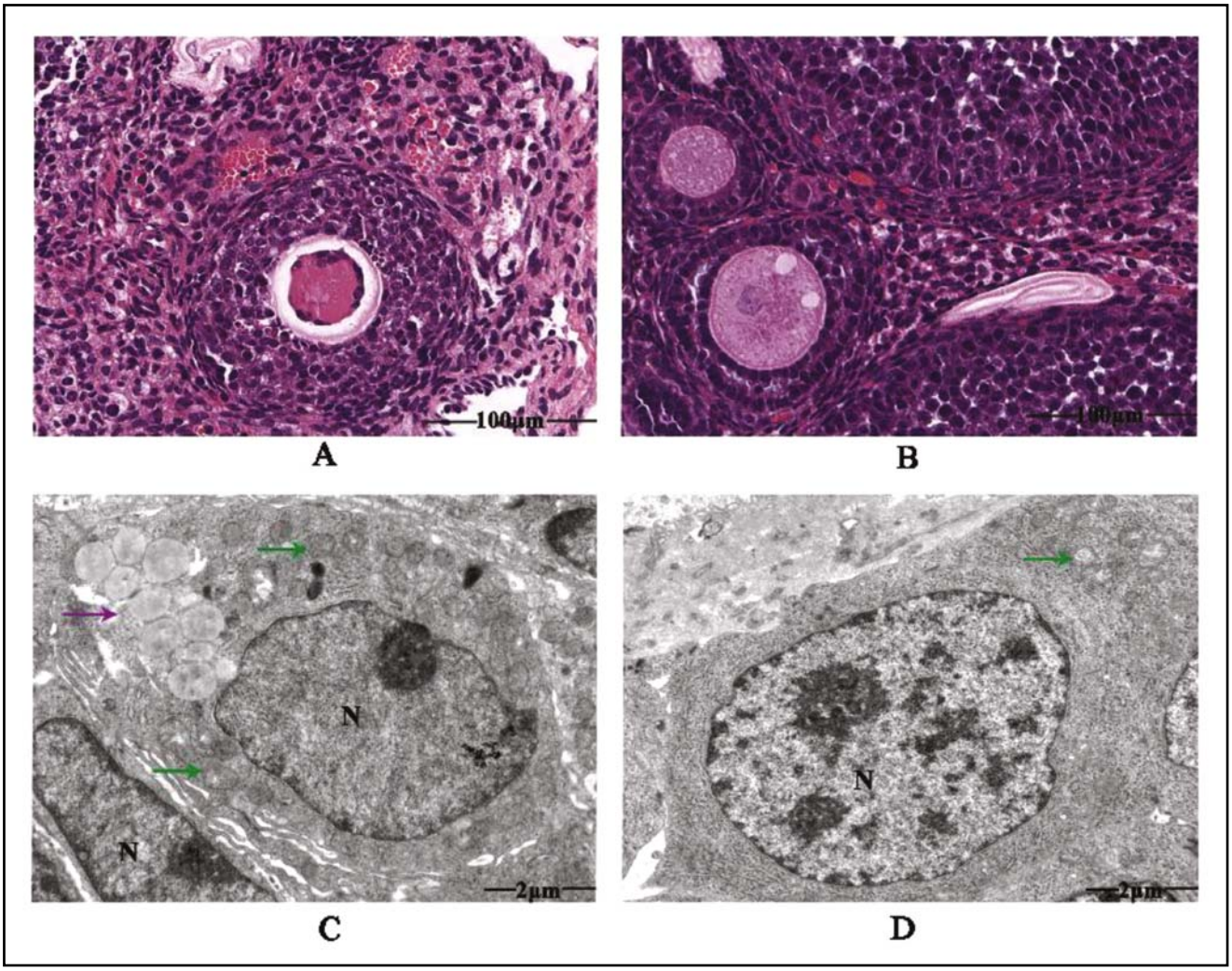

Fig. 3. Comparison of ovarian morphology between obese and control mice on postnatal day 45. Effects of high fat diet during pubertal development period on ovarian morphology in female mice on postnatal day 45. A: the ovary of HFD female mice (HE, 800×); B: the ovary of CONT female mice (HE, 800×); C: the ovary of HFD female mice (transmission electron microscope, 10000×) ; D: the ovary of CONT female mice (transmission electron microscope, 10000×). N: nucleus; Purple arrows: lipid droplets; Green arrows: mitochondria. HFD: high-fat diet; CONT: control. HE: haematoxylin and eosin.

Transmission electron microscopy

Three ovaries from each group were prepared for transmission electron microscopy. The ovaries were cut into fragments (1 mm × 1 mm × 1 mm), fixed in 0.1 M phosphate-buffered saline (PBS), pH 7.2, containing 2.5% glutaraldehyde, post-fixed in 1% osmium tetroxide, dehydrated in a series of ethanol and acetone solutions, and embedded in Epon 812 Resin. Next, the tissue blocks were sectioned using an LKB ultramicrotome, and the sections were stained with uranyl acetate followed by lead citrate, observed under an H-600 transmission electron microscope, and photographed.

Enzyme-linked immunosorbent assay

Serum estradiol (E2) and luteinizing hormone (LH) levels were measured by enzyme-linked immunosorbent assay (ELISA), according to the manufacturer's instructions. The detection range of the E2 ELISA (Shanghai Enzyme-Linked Biotechnology Co., Ltd., Shanghai, China) was 3.75–120 pg/mL, whereas that of the LH ELISA (Shanghai Enzyme-Linked Biotechnology Co., Ltd.) was 0.25–8 mIU/mL. Each sample was tested in duplicate.

Hematoxylin–eosin staining

Hematoxylin–eosin staining was performed as previously described) (Nichols *et al.* 2005). Three ovaries from each group were fixed in 4% paraformaldehyde, rinsed with water, and stored in 70% ethanol. The tissues were subsequently embedded in paraffin wax, sectioned to a thickness of 5 μm using a rotary microtome, collected on microscope slides, and dried at 56°C for 24 h. Next, the sections were passed through xylene solutions and rehydrated in a graded series of ethanol solutions. The sections were subsequently stained with hematoxylin, rinsed with water, differentiated in 1% acid alcohol for 30 s, and rinsed with water. Lastly, the sections were counterstained with eosin, dehydrated in

a graded series of ethanol solutions, and passed through xylene. The sections were cover-slipped, observed under a light microscope, and photographed.

Immunohistochemical analysis

Immunohistochemical staining was performed. The hypothalami were sectioned to a thickness of 4 μm, and the sections between two distinct anatomic locations within the mediobasal hypothalamus (MBH, –1.3 and –1.8 from the bregma, the posterior two-thirds of the hypothalamic arcuate nucleus) were analyzed as previously described (Zhai *et al.* 2018). Three sections were randomly selected from each group and subjected to immunohistochemical staining using the EliVision Plus Kit (Fuzhou Maixin Biotech Co., Ltd., Fuzhou, China). Antigen retrieval was performed in an autoclave at 100 °C for 20 min in antigen retrieval buffer, and the anti-GnRH rabbit monoclonal antibody (cat. no. ab5617, 1:100; Abcam, Cambridge, UK) was used. The sections were counterstained with hematoxylin. The integrated optical density/area (IOD/area), which was determined by ImageJ software (National Institutes of Health, Bethesda, MD, USA), was used to quantify the relative GnRH expression.

Western blotting

Western blotting was performed as previously described (Zhai *et al.* 2018). The hypothalami were washed twice in ice-cold PBS, pH 7.5, and dissociated in radioimmunoprecipitation assay buffer. The samples were centrifuged, and the protein lysates (50 mg) were separated by 10% sodium dodecyl sulfate–polyacrylamide gel electrophoresis, followed by the transfer of proteins to membranes. After blocking, the membranes were incubated with an anti-MKRN3 antibody (cat. no. A16073, 1:1000; ABclonal, Wuhan, China), anti-kisspeptin antibody (cat. no. ab19028, 1:500; Abcam, Boston, MA, USA), anti-GPR54 antibody (cat. no. PA5-49719, 1:500; Invitrogen, Waltham, MA, USA), and anti-GnRH antibody (cat. no. ab16216, 1:500; Abcam). The membranes were washed and incubated with secondary antibodies (1:5000; ABclonal). The immunoreactive proteins were detected using standard enhanced chemiluminescence reagents. Each sample was tested at least in triplicate.

RNA isolation and quantitative PCR analysis

Total mRNA was extracted from the hypothalami using TRIzol Reagent (TaKaRa Biotechnology Co., Ltd., Dalian, China). The quantity and integrity of RNA were characterized by UV spectrophotometry. Semi-quantitative reverse transcription was performed using the PrimeScript RT Reagent Kit with DNA Eraser (TaKaRa Biotechnology Co., Ltd.), whereas qPCR was performed using the SYBR Green PCR Kit (TaKaRa Biotechnology Co., Ltd.) in conjunction with the Quant Studio 6 Flex Real-Time PCR System (Applied Biosystems, Waltham, MA, USA). The gene-specific primers (Table 1) were designed by Beijing Dinguo Changsheng Biotechnology Co., Ltd. (Beijing, China). The initial denaturation was carried out at 95°C for 30 s, followed by 40 cycles at 95°C for 5 s and 60°C for 30 s. The analysis of gene expression levels was performed by the $2^{-\Delta Ct}$ method. The raw data were normalized to the housekeeping gene (β-actin or U6). All reactions were performed in duplicate.

Statistical analysis

All statistical analyses were performed with SPSS 25.0 software (SPSS Inc., Chicago, IL, USA). The measurement data were described as mean ± SD. The independent samples t-test was used to compare differences between the two groups. The inspection level was taken at $\alpha = 0.05$.

RESULTS

Comparison of body weight between obese and control mice from postnatal day 21 to 45

As shown in Figure 1, the body weight of HFD mice was significantly greater than that of CONT mice on P21 ($p < 0.05$, n = 12), indicating that the obesity model was successfully established. The body weight of HFD mice was significantly greater than that of CONT mice on P45 ($p < 0.05$).

Comparison of body fat percentage, reproductive organ weight, sex hormone levels, vaginal opening time, and ovarian morphology between obese and control mice on postnatal day 45

As shown in Table 2, compared with CONT mice, the body weight and body fat (%) of HFD mice increased significantly on P45 ($p < 0.05$). The weights of the ovaries and uterus, as well as the ovarian weight coefficient and uterine weight coefficient, of HFD mice were significantly greater than that of CONT mice on P45 ($p < 0.05$). The serum E2 and LH levels were measured by ELISA, as shown in Table 2, and serum E2 and LH levels of HFD mice were significantly higher than those of CONT mice on P45 ($p < 0.05$, n = 8).

As shown in Figure 2, the average vaginal opening times of HFD and CONT mice were 34.3 ± 3.1 and 40.1 ± 3.6 days, respectively, indicating that the vagina opened significantly earlier in HFD mice than that in CONT mice ($p < 0.05$, n = 12).

Hematoxylin–eosin staining and transmission electron microscopy were used to examine ovarian morphology on P45 (Figure 3). On P45, by hematoxylin–eosin staining, the ovarian follicular cavity of HFD mice (Figure 3A) was larger than that of CONT mice (Figure 3B). In addition, in HFD mice, follicular fluid was abundant, granulosa cells were arranged in a disordered pattern, the number of granulosa cells was decreased, and the number of corpus lutea was increased. By electron microscopy, the nuclear chromatin was uniform, and the structure of the ovaries

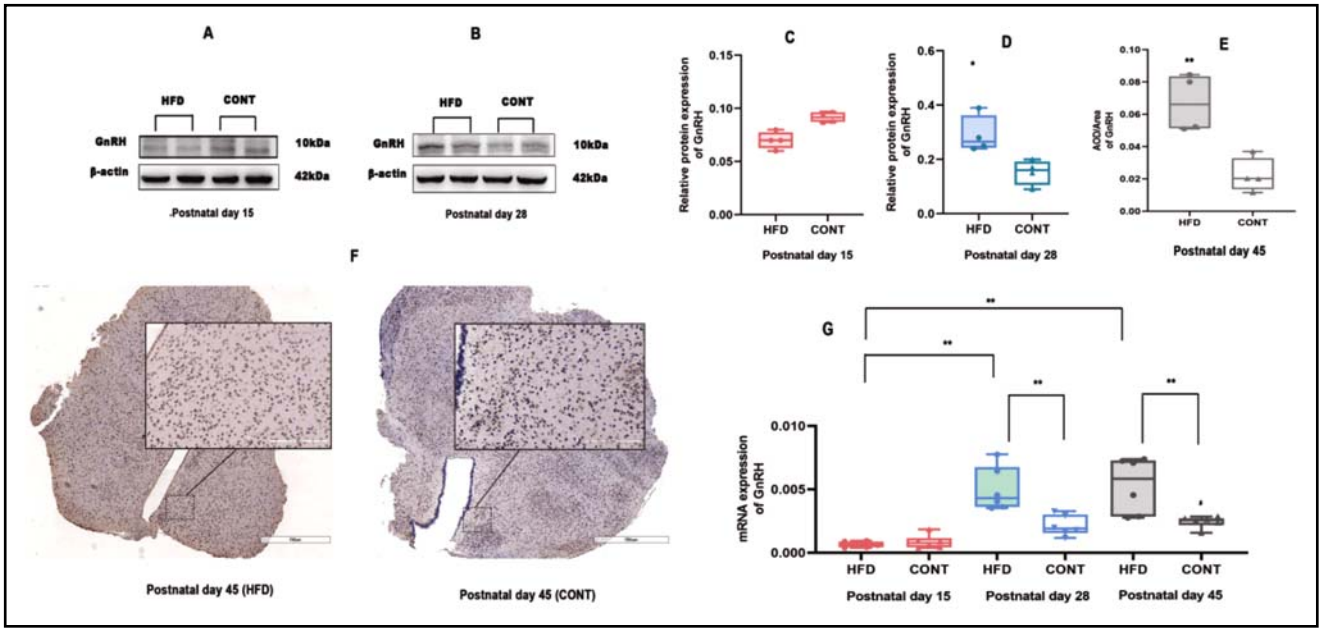

Fig. 4. Comparison of GnRH protein and mRNA levels between obese and control mice on postnatal days 15, 28, 45. Representative western blots using antibodies against GnRH in hypothalamus of female mice on postnatal day 15 and 28 (A, B). Positive staining (brown staining) was stronger in the HFD group as compared to the CONT group (F). Measurements of GnRH on postnatal day 15 (C), 28 (D) and 45 (E). Data were presented as mean±SD, n = 4. The bar graphs G show the results of the measurement of GnRH mRNA expression on postnatal day 15, 28, and 45. Data are presented as mean±SD, n = 6. *P < 0.05 , **P < 0.01 as compared to the control. #P < 0.05 as compared to the CONT (Postnatal day15). GnRH: gonadotropin-releasing hormone; HFD: high-fat diet; CONT: control. SD: standard deviation.IOD: Integrated Optical Density.

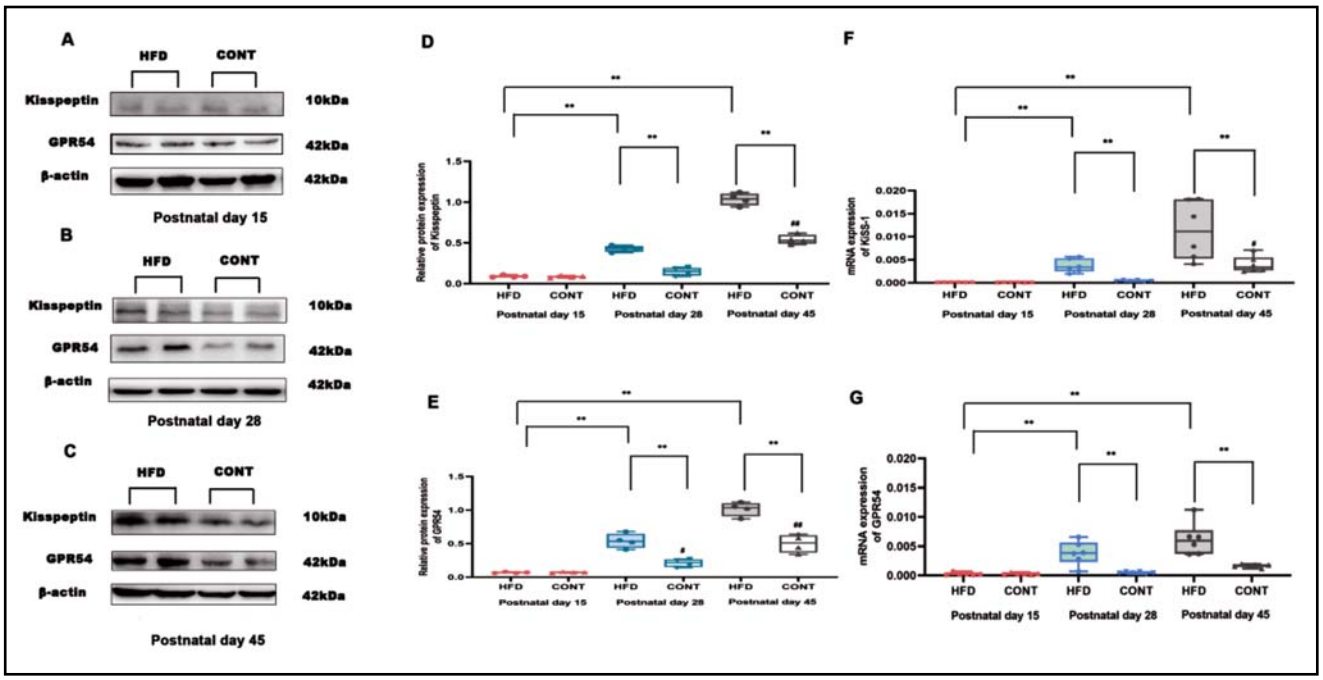

Fig. 5. Comparison of kisspeptin, GPR54 protein and mRNA levels between obese and control mice on postnatal days 15, 28 and 45. Representative western blots using antibodies against kisspeptin and GPR54 in hypothalamus of female mice on postnatal days 15, 28 and 45 (A, B, C). Measurements of kisspeptin (D), GPR54 (E) on postnatal day 15, 28and 45. Data were presented as mean±SD, n = 4. The bar graphs show the results of the measurement of KiSS-1 and GPR54 mRNA expression on postnatal day 15, 28 and 45 (F,G) , respectively. Data are presented as mean±SD, n = 6. *P < 0.05, **P < 0.01 as compared to the control. #P < 0.05, ##P < 0.01 as compared to the CONT (Postnatal day 15). GPR54: G protein-coupled receptor 54; HFD: high-fat diet; CONT: control. SD: standard deviation.

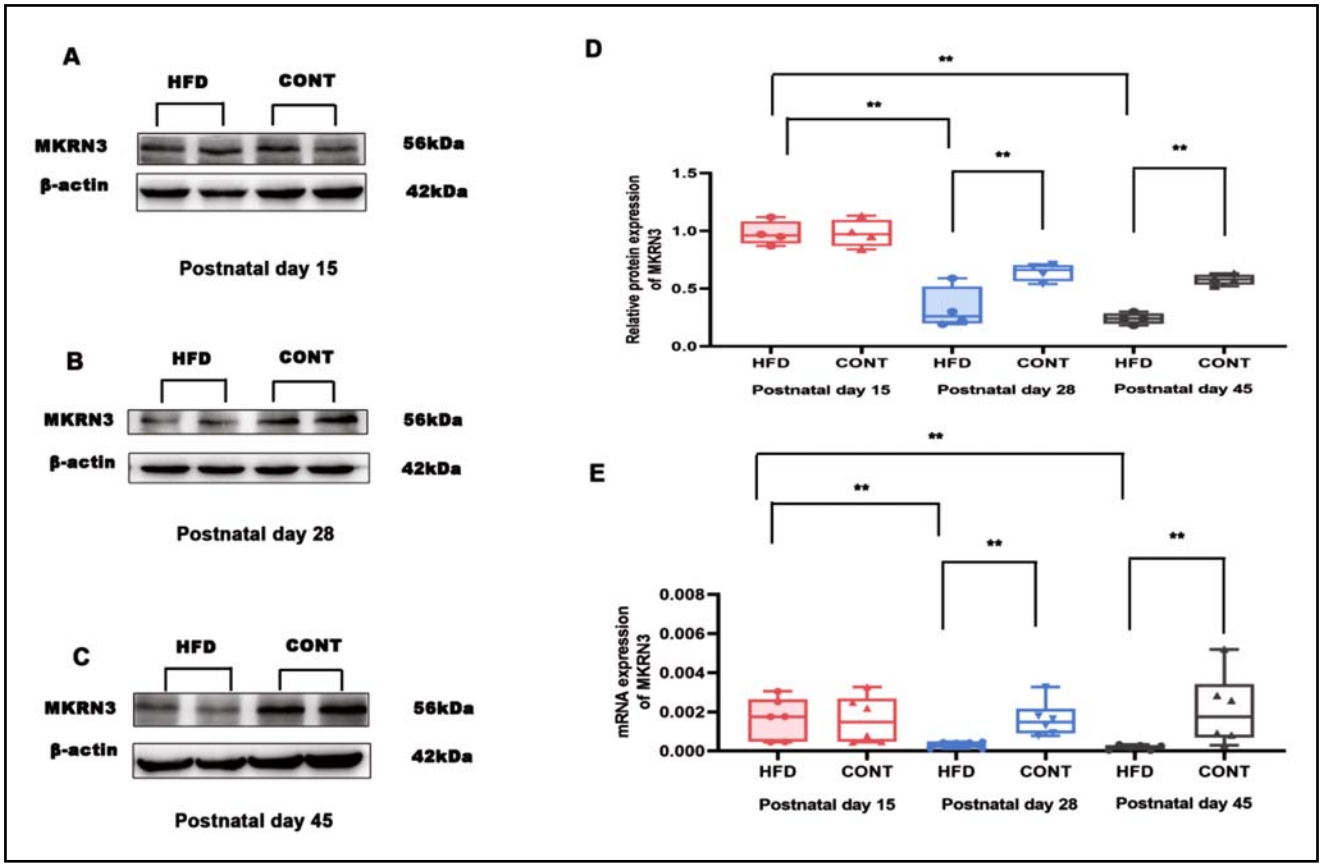

Fig. 6. Comparison of MKRN3 protein and mRNA levels between obese and control mice on postnatal days 15, 28 and 45. Representative western blots using antibodies against MKRN3 in hypothalamus of female mice on postnatal day 15, 28 and 45 (A, B, C). Measurements of MKRN3 on postnatal day 15, 28, and 45 (D). Data were presented as mean±SD, n = 4. The bar graphs show the results of the measurement of MKRN3 mRNA expression on postnatal day 15, 28 and 45 (E). Data were presented as mean±SD, n = 6. *$P < 0.05$, **$P < 0.01$ as compared to the control. MKRN3: makorin ring finger protein 3; HFD: high-fat diet; CONT: control. SD: standard deviation.

was intact. However, there were many mitochondria in the granulosa cells of HFD mice (Figure 3C), and numerous lipid droplets were observed in the cytoplasm and stroma.

Comparison of GnRH protein and mRNA levels between obese and control mice on postnatal days 15, 28, and 45

The GnRH protein level in the hypothalamus was examined by western blotting on P15 and 28 and by immunohistochemical staining on P45 (Figure 4). On P15, no significant difference in GnRH protein expression between HFD and CONT mice was noted ($p > 0.05$, n = 4). On P28, compared to CONT mice, GnRH protein expression in HFD mice was significantly increased (Figure 4D, $p < 0.05$, n = 4). On P45, HFD mice showed stronger GnRH-labeling intensity (brown precipitates) compared with CONT mice (Figure 4F). By immunohistochemical analysis, it was observed that the GnRH level increased compared to the CONT-group (Figure 4E, $p < 0.05$, n = 4).

The GnRH mRNA level in the hypothalamus was also examined by qPCR on P15, P28, P45. On P15, no significant difference in GnRH expression between HFD and CONT mice was noted (Figure 4G) ($p > 0.05$, n = 6). However, compared to CONT mice, GnRH expression in HFD mice increased on P28 and 45 significantly compared to the CONT-group, respectively ($p < 0.05$, n = 6). And compared to P15, GnRH mRNA level on P28 and 45 increased significantly in HFD mice ($p < 0.01$). Compared to P15, GnRH mRNA level on P45 increased significantly in CON mice ($p < 0.01$).

Comparison of kisspeptin and GPR54 protein and mRNA levels between obese and control mice on postnatal days 15, 28, and 45

The kisspeptin and GPR54 protein levels in the hypothalamus were examined by western blotting. On P15, no significant differences in the levels of kisspeptin and GPR54 between HFD and CONT mice were detected ($p > 0.05$, n = 4) (Figure 5A, D, E, Supplementary Figure 1, 2, 3 online www.nel.edu). On P28 and 45, compared to CONT mice, kisspeptin, and GPR54 protein expression in HFD mice was significantly increased (Figure 5D, E) ($p < 0.05$, n = 4). Compared to P15, kisspeptin level on P45 increased significantly in CON mice ($p < 0.01$). And compared to P15, GPR54 level on P28 and 45 increased significantly in CON mice ($p < 0.05$).

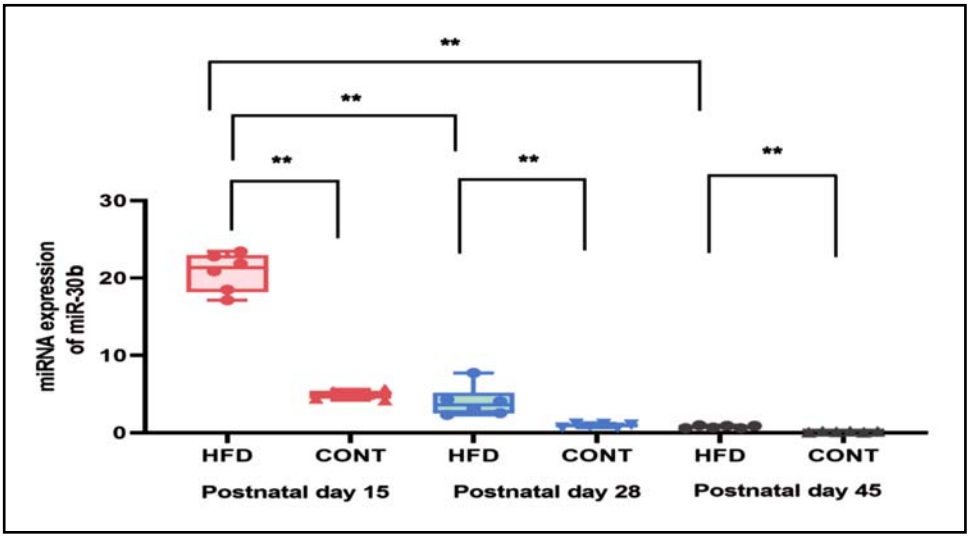

Fig. 7. Comparison of miR-30b between obese and control mice on postnatal days 15, 28, 45. Data are presented as mean±SD, n = 6, $^{**}P < 0.01$ as compared to the control. miR-30b:microRNA-30b; HFD: high-fat diet; CONT: control. SD: standard deviation.

The KiSS-1 and GPR54 mRNA levels in the hypothalamus were also examined by qPCR (Figure 5F, G). On P15, no significant differences in the levels of KiSS-1 and GPR54 in HFD and CONT mice were noted ($p > 0.05$, n = 6). On P28 and 45, compared to CONT mice, KiSS-1 and GPR54 expression in HFD mice increased significantly compared to that of the CONT-group, respectively ($p < 0.01$, n = 6). And compared to P15, KiSS-1 and GPR54 mRNA level on P28 and 45 increased significantly in HFD mice ($p < 0.01$). Compared to P15, KiSS-1 mRNA level on P45 increased significantly in CON mice ($p < 0.05$).

Comparison of MKRN3 protein and mRNA levels between obese and control mice on postnatal days 15, 28, and 45

The MKRNS protein level was examined by western blotting (Figure 6A, B, C, Supplementary Figure 1, 2, 3 online www.nel.edu), and the levels of MKRNS mRNA (Figure 6E) were examined by qPCR. On P15, no significant difference in the MKRN3 protein level between HFD and CONT mice was detected (Figure 6D). On P28 and 45, the MKRN3 protein level in HFD mice was significantly lower than that in CONT mice (Figure 6D) ($p < 0.05$, n = 4).

On P15, no significant difference in the MKRN3 mRNA level between HFD and CONT mice ($p > 0.05$). However, MKRN3 mRNA expression in HFD mice decreased significantly compared to the CONT-group value on P28 and P45, respectively (Figure 6E) ($p < 0.01$, n = 6). And compared to P15, MKRN3 mRNA level on P28 and 45 decreased significantly in HFD mice ($p < 0.01$).

Comparison of miR-30b level between obese and control mice on postnatal days 15, 28, and 45

On P15, miR-30b expression in HFD mice increased significantly compared to the CONT-group ($p < 0.01$, n = 6). On P28 and 45, miR-30b expression in HFD mice increased obviously compared to the CONT-group, respectively (Figure 7, $p < 0.01$, n = 6). But compared to P15, miR-30b level on P28 and 45 decreased significantly in HFD mice ($p < 0.01$).

DISCUSSION

Feeding C57BL/6J mice a diet that is high in fat (60% of total calories) is a commonly used strategy to induce experimental obesity. In this study, we established an obesity model using this approach; however, different investigators have used different strategies to study prepubertal obesity (Ribaroff *et al.* 2017; Connor *et al.* 2012). High-fat diet exposure early in life (pregnancy, lactation, or childhood) often leads to prepubertal obesity. In this study, we examined prepubertal obesity after HFD exposure during lactation and childhood after considering the results of previous studies. Ribaroff *et al.* (2017) reported that HFD exposure of mothers (pregnancy or lactation) could affect the metabolism of offspring. To investigate the effects of prepubertal obesity on puberty onset and to increase the exposure time, offspring at post-weaning were fed a HFD, similar to the study of Connor *et al.* (2012). Furthermore, during lactation or childhood, offspring are directly exposed to the diet, thereby eliminating the absorption of nutrients by the placenta during gestation. According to the definition of obesity (Xu *et al.* 2019; Sánchez-Garrido *et al.* 2015), the body weight and body fat percentage of HFD mice were significantly higher than those of CONT mice from P21 to 45 (childhood period), indicating successful establishment of the obesity model.

The opening of the vagina is an indicator of the onset of puberty (Ullah *et al.* 2017). In this study, compared with CONT mice, the opening of the vagina in HFD mice occurred significantly earlier, consistent with the results of a previous study (Venancio *et al.* 2017). To investigate the effects of HFD exposure on

reproductive function, hematoxylin–eosin staining and transmission electron microscopy were used to observe ovarian morphology. Compared with CONT mice, follicular development was normal and the number of corpus lutea was increased in P45 mice fed a HFD. The ovarian morphology was unremarkable, although there were many mitochondria in granulosa cells of HFD mice. Compared with CONT mice, reproductive development and puberty onset occurred sooner in HFD mice than in CONT mice, confirming that prepubertal obesity can lead to early-onset puberty.

The mechanism of early-onset puberty in obese mice is still unclear. Neuroendocrine changes before puberty onset may play an important role, and our earlier study had demonstrated that elevated sex hormone levels may be the key factor (Zhai *et al.* 2015). To examine the neuroendocrine changes before puberty onset, we selected three time points, namely, P15 (prepuberty) (Messina *et al.* 2016), P28 (puberty onset) (Kaviani *et al.* 2016), and P45 (puberty completion).

On P45, we measured serum E2 and LH levels and observed that the levels of both sex hormones increased significantly. The E2 level is regulated by the LH level, which can initiate early reproductive development and puberty in obese mice, consistent with the results of previous studies (Li *et al.* 2012; Ullah *et al.* 2019). In addition, sex hormone secretion is regulated by the HPG axis. During puberty initiation, the GnRH level increases to act on the pituitary, which increases the levels of LH and other sex hormones and promotes puberty initiation and reproductive development. We examined GnRH mRNA and protein levels in the hypothalamus on P15, 28, and 45 and observed that the GnRH levels in HFD mice were significantly higher than those in CONT mice on P28 and 45, and compared to P15, GnRH mRNA level on P28 and 45 increased, which indicated that the GnRH level increased before puberty onset, which may be the reason for the increase in E2 and LH levels.

What can regulate GnRH during prepuberty? In recent years, the relationship between miRNA expression and GnRH secretion has received significant attention. MiRNAs are small endogenous non-coding single-stranded RNAs comprised of 19–22 nucleotides (Lee *et al.* 1993). In a study of the Dicer gene (a key endonuclease for miRNA formation), which described its deletion in hypothalamic GnRH-expressing neurons, hypogonadal dysfunction and infertility were observed (Messina *et al.* 2016; Chekulaeva *et al.* 2009), indicating that miRNAs play key roles in puberty initiation and reproductive development (Chekulaeva *et al.* 2009). MiR-30 is one example of an miRNA that affects puberty initiation (Heras *et al.* 2019). The miR-30 family consists of five members, namely, miR-30a, miR-30b, miR-30c, miR-30d, and miR-30e (Sangiao-Alvarellos *et al.* 2014). Among these, miR-30b was selected for further study because of the relationship between miR-30b regulation and MKRN3 expression. MKRN3 is an essential component of the gene regulatory network that initiates puberty in mammals. MiR-30b binds to the 3' untranslated region of MKRN3 and directly inhibits MKRN3 secretion, thereby affecting puberty initiation (Heras *et al.* 2019). Several studies have reported that MNRN3 can regulate pubertal development through GnRH (Heras *et al.* 2019; Atay *et al.* 2012). For example, Abreu *et al.* demonstrated that MKRN3 regulates pubertal onset and GnRH release by inhibiting kisspeptin expression in the hypothalamus (Abreu *et al.* 2020), indicating that kisspeptin is a mediator of MNRN3-induced GnRH secretion. In this study, the expression of miR-30b increased before puberty onset, which inhibited the expression of MKRN3; reversed the inhibitory effect of MKRN3 on the kisspeptin/GPR54/GnRH pathway; increased the expression of kisspeptin, GPR54, and GnRH; and promoted the secretion of E2 and LH, thereby leading to puberty onset.

In this study, we investigated miR-30b, MNRN3, kisspeptin, and GPR54 expression in the hypothalamus during the development of puberty. On P15 (prepuberty), miR-30b and MNRN3 expression in HFD mice increased compared with CONT mice, while no significant differences in the levels of the other genes were noted. In addition, no significant differences in the protein levels of MKRN3, kisspeptin, GPR54, and GnRH between the two groups were detected. However, on P28, beside miR-30b, the gene and protein expression of MKRN3, kisspeptin, GPR54, and GnRH changed in the HFD compared to the control mice. And we also found compared to P15, miR-30b level of HFD mice increased on P28. Thus, we thought that the changes of gene and protein expression of MKRN3, kisspeptin, GPR54, and GnRH followed with the change of miR-30b, and the change occurred earlier in HFD than in control mice.

On P28, miR-30b increased, MNRN3 expression decreased, while kisspeptin/GPR54 and GnRH expression increased in mice fed a HFD. As the discussion above, an inhibit role of miR-30b on MNRN3 were found. The decreased level of MNRN3 may release the inhibiting effect on kisspeptin, which promote the expression of kisspeptin/GPR54 and GnRH. And an enhanced inhibiting effect of miR-30b in HFD mice were found than in control mice because of the increase phenomenon firstly found in HFD mice on P15 compared to the control mice. Similar, compared to P15, more gene level changes of MNRN3, kisspeptin/GPR54 and GnRH were found in HFD mice than in control mice on P28. So we thought that before the development of puberty, the increase in the levels of miR-30b, kisspeptin, GPR54, GnRH, and decrease in the level of MKRN3, occurred earlier in obese mice than in normal mice, which may be the main reason for the higher sex hormone levels, the earlier opening of the vagina in HFD mice. Similar changes in miR-30b, MKRN3, kisspeptin, GPR54, and GnRH expression were also observed on P45, which means the change

of the genes and proteins in HFD mice hold on till P45 (puberty completion). Whether the changes will hold in the followed days, we were not sure, more study should be done to verify it.

There was some limitation in this study. Firstly, we did not found the exact time point for the increasing of miR-30b in HFD mice compared to the CONT mice. On P15, compared to the CONT mice, miR-30b increased already. Secondly, the weight of HFD mice were higher than normal mice from day 21, but some study didn't find a difference between high fat fed mice and normal diet fed mice until day 27-29. We think the main reason may be the difference batch of mice and the status of dam mice. There were possible animal species and status factors in the animal study.

Taken collectively, prepubertal obesity induced by HFD during lactation and post-weaning may advance the time of pubertal onset in female mice. Before the development of puberty, the increase in the levels of miR-30b may inhibit the level of MKRN3, then kisspeptin, GPR54 and GnRH expression increased (occurred earlier in HFD mice than in normal mice), which may be the main reason for the higher sex hormone levels, and the earlier opening of the vagina in HFD mice.

DECLARATION OF INTEREST, FUNDING AND ACKNOWLEDGEMENTS

Ethical Approval

All experimental procedures were conducted in accordance with the institutional guidelines for the care and use of laboratory animals at China Medical University (Shenyang, China) (CMU2019186) and the National Institutes of Health Guide for Care and Use of Laboratory Animals (publication no. 85-23, revised 1985) with experimental protocol no. SYXK (Liao) 2018-0008.

Declaration of interest

The authors have no relevant financial or non-financial interests to disclose.

Authors' Contributions

M. S. and L. Z. wrote the main manuscript text; L. Z. conceived and designed the experiments; M. S., S. R., Y. Z. and Q. Y. performed the experiments and analyzed the data; L. Z. review and edited the paper. All authors reviewed the manuscript.

Fundings

This work was supported by the National Natural Science Foundation of China (grant no: 81872640, 81671515). Science and Technology Planning Project of Liaoning Province (2021-MS-217).

Acknowledgements

Not applicable

REFERENCES

1 Abreu AP, Kaiser UB (2016). Pubertal development and regulation. Lancet Diabetes Endocrinol. **4**: 254–264.
2 Abreu AP, Toro CA, Song YB, Navarro VM, Bosch MA, Eren A, et al. (2020). MKRN3 inhibits the reproductive axis through actions in kisspeptin-expressing neurons. J Clin Invest. **130**: 4486–4500.
3 Agbu P, Carthew RW (2021). MicroRNA-mediated regulation of glucose and lipid metabolism. Nat Rev Mol Cell Biol. **6**: 425–438.
4 Atay Z, Turan S, Guran T, Furman A, Bereket A (2012). The prevalence and risk factors of premature thelarche and pubarche in 4- to 8-year-old girls. Acta Paediatr. **101**: e71–e75.
5 Biro FM, Pajak A, Wolff MS, Pinney SM, Windham GC, Galvez MP, et al. (2018). Age of Menarche in a Longitudinal US Cohort. J Pediatr Adolesc Gyneco. **31**: 339–345.
6 Chekulaeva M, Filipowicz W (2009). Mechanisms of miRNA-mediated post-transcriptional regulation in animal cells. Curr Opin Cell Biol. **21**: 452–460.
7 Cheng TS, Day FR, Lakshman R, Ong KK (2020). Association of puberty timing with type 2 diabetes: a systematic review and meta-analysis. PLoS Med. **17**: e1003017.
8 Collaborative Group on Hormonal Factors in Breast Cancer (2012). Menarche, menopause, and breast cancer risk: individual participant meta-analysis, including 118 964 women with breast cancer from 117 epidemiological studies. Lancet Oncol. **13**: 1141–1151.
9 Colich NL, Platt JM, Keyes KM, Sumner JA, Allen NB, McLaughlin KA (2020). Earlier age at menarche as a transdiagnostic mechanism linking childhood trauma with multiple forms of psychopathology in adolescent girls. Psychol Med. **7**: 1090–1098.
10 Connor KL, Vickers MH, Beltrand J, Meaney MJ, Sloboda DM (2012). Nature, nurture or nutrition? Impact of maternal nutrition on maternal care, offspring development and reproductive function. J Physiol. **9**: 2167–80.
11 Eckert-Lind C, Busch AS, Petersen JH, Biro FM, Butler G, Bräuner EV, et al. (2020). Worldwide secular trends in age at pubertal onset assessed by breast development among girls: a systematic review and meta-analysis. JAMA Pediatr. **174**: e195881.
12 Greenspan LC, Lee MM (2018). Endocrine disrupters and pubertal timing. Curr Opin Endocrinol Diabetes Obes. **25**: 49–54
13 Harter CJL, Kavanagh GS, Smith JT (2018). The role of kisspeptin neurons in reproduction and metabolism. J Endocrinol. **238**: R173–R183.
14 Herbison AE (2016). Control of puberty onset and fertility by gonadotropin-releasing hormone neurons. Nat Rev Endocrinol. **12**: 452–466.
15 Heras V, Sangiao-Alvarellos S, Manfredi-Lozano M, Sanchez-Tapia MJ, Ruiz-Pino F, Roa J, et al. (2019). Hypothalamic miR-30 regulates puberty onset via repression of the puberty-suppressing factor, Mkrn3. PLoS Biol. **17**: e3000532.
16 Huang A, Reinehr T, Roth CL (2020). Connections Between Obesity and Puberty: Invited by Manuel Tena-Sempere, Cordoba. Curr Opin Endocr Metab Res. **14**: 160–168.
17 Huang A, Roth CL (2021). The link between obesity and puberty: what is new? Curr Opin Pediat. **33**: 449–457.
18 Jacobsen BK, Oda K, Knutsen SF, Fraser GE (2009). Age at menarche, total mortality and mortality from ischaemic heart disease and stroke: the Adventist Health Study, 1976-88. Int J Epidemiol. **38**: 245–252.
19 Kaviani R, Londono I, Parent S, Moldovan F, Villemure I (2016). Growth plate cartilage shows different strain patterns in response to static versus dynamic mechanical modulation. Biomech Model Mechanobiol. **15**: 933–946.
20 Krieger N, Kiang MV, Kosheleva A, Waterman PD, Chen JT, Beckfield J (2015). Age at menarche: 50-year socioeconomic trends among US-born black and white women. Am J Public Health. **105**: 388–397.
21 Lee RC, Feinbaum R, Ambros V (1993). The C. elegans heterochronic gene lin-4 encodes small RNAs with antisense complementarity to lin-14. Cell. **75**: 843–854.
22 Li XF, Lin YS, Kinsey-Jones JS, O'Byrne KJ (2012). High-fat diet increases LH pulse frequency and kisspeptin-neurokinin B expression in puberty-advanced female rats. Endocrinology. **153**: 4422–4431.

23 Livadas S, Chrousos GP (2019). Molecular and Environmental Mechanisms Regulating Puberty Initiation: An Integrated Approach. Front Endocrinol (Lausanne). **10**: 828.
24 Messina A, Langlet F, Chachlaki K, Roa J, Rasika S, Jouy N, et al. (2016). A microRNA switch regulates the rise in hypothalamic GnRH production before puberty. Nat Neurosci. **19**: 835–844.
25 Nichols SM, Bavister BD, Brenner CA, Didier PJ, Harrison RM, Kubisch HM (2005). Ovarian senescence in the rhesus monkey (Macaca mulatta). Hum Reprod. **20**: 79–83.
26 Ribaroff GA, Wastnedge E, Drake AJ, Sharpe RM, Chambers TJG (2017). Animal models of maternal high fat diet exposure and effects on metabolism in offspring: a meta-regression analysis. Obes Rev. **6**: 673–686.
27 Sánchez-Garrido MA, Ruiz-Pino F, Manfredi-Lozano M, Leon S, Heras V, Castellano JM, et al. (2015). Metabolic and Gonadotropic Impact of Sequential Obesogenic Insults in the Female: Influence of the Loss of Ovarian Secretion. Endocrinology. **156**: 2984–2998.
28 Sangiao-Alvarellos S, Pena-Bello L, Manfredi-Lozano M, Tena-Sempere M, Cordido F (2014). Perturbation of hypothalamic microRNA expression patterns in male rats after metabolic distress: impact of obesity and conditions of negative energy balance. Endocrinology. **155**: 1838–1850.
29 Terasawa E, Fernandez DL (2001). Neurobiological mechanisms of the onset of puberty in primates. Endocr Rev. **22**: 111–151.
30 Ullah R, Raza A, Rauf N, Shen Y, Zhou YD, Fu J (2019). Postnatal Feeding With a Fat Rich Diet Induces Precocious Puberty Independent of Body Weight, Body Fat, and Leptin Levels in Female Mice. Front Endocrinol (Lausanne). **10**: 758.
31 Ullah R, Su Y, Shen Y, Li C, Xu X, Zhang J, et al. (2017). Postnatal feeding with high-fat diet induces obesity and precocious puberty in C57BL/6J mouse pups: a novel model of obesity and puberty. Frontiers of medicine. **11**: 266–276.
32 Venancio JC, Margatho LO, Rorato R, Rosales RRC, Debarba LK, Coletti R, et al. (2017). Short-Term High-Fat Diet Increases Leptin Activation of CART Neurons and Advances Puberty in Female Mice. Endocrinology. **158**: 3929–3942.
33 Vogelezang S, Bradfield JP, Ahluwalia TS, Curtin JA, Lakka TA, Grarup N, et al. (2020). Novel loci for childhood body mass index and shared heritability with adult cardiometabolic traits. PLoS Genet. **7**: e1008718.
34 Wang H, Xue H, Du S, Zhang J, Wang Y, Zhang B (2017). Time trends and factors in body mass index and obesity among children in China: 1997-2011. Int J Obes (Lond). **4**: 964–970.
35 Wood CL, Lane LC, Cheetham T (2019). Puberty: Normal physiology (brief overview). Best Pract Res Clin Endocrinol Metab. **33**: 101265.
36 World Health Organization. Obesity and overweight [EB]. https://www.who.int/ news- room/fact-sheets/detail/obesity-and-overweight. Accessed 21 October 2022
37 Wu XQ, Li XF, Jin WW, Li HY (2012). Effects of obesity on pubertal initiation and reproductive function in female rats. Zhonghua Yi Xue Za Zhi. **92**: 932–934.
38 Xu HQ, Sun JM, Ma GS (2021). Promoting childhood obesity prevention and control through social environment optimization. Chinese Journal of School Health. **42**: 1601–1604.
39 Xu L, Nagata N, Chen G, Nagashimada M, Zhuge F, Ni Y, et al. (2019). Empagliflozin reverses obesity and insulin resistance through fat browning and alternative macrophage activation in mice fed a high-fat diet. BMJ Open Diabetes Res Care. **7**: e000783.
40 Yang Y, Smith DL Jr, Keating KD, Allison DB, Nagy TR (2014). Variations in body weight, food intake and body composition after long-term high-fat diet feeding in C57BL/6J mice. Obesity (Silver Spring). **22**: 2147–2155.
41 Zhai L, Liu J, Zhao J, Liu J, Bai Y, Jia L, Yao X (2015). Association of Obesity with Onset of Puberty and Sex Hormones in Chinese Girls: A 4-Year Longitudinal Study. PLoS One. **10**: e0134656.
42 Zhai L, Zhao J, Zhu Y, Liu Q, Niu W, Liu C, et al. (2018). Downregulation of leptin receptor and kisspeptin/GPR54 in the murine hypothalamus contributes to male hypogonadism caused by high-fat diet-induced obesity. Endocrine. **62**: 195–206.
43 Zhou J, Zhang F, Zhang S, Li P, Qin X, Yang M, et al. (2022). Maternal pre-pregnancy body mass index, gestational weight gain, and pubertal timing in daughters: A systematic review and meta-analysis of cohort studies. Obes Rev. **23**: e13418.

Publisher Note:
Open Access Full text PDF with Supplementary Figures 1,2,3 online:
www.nel.edu
Vol. 44, Issue 3, 2023

SUPPLEMENTARY FIGURE 1 - FULL SIZE WESTERN BLOTS

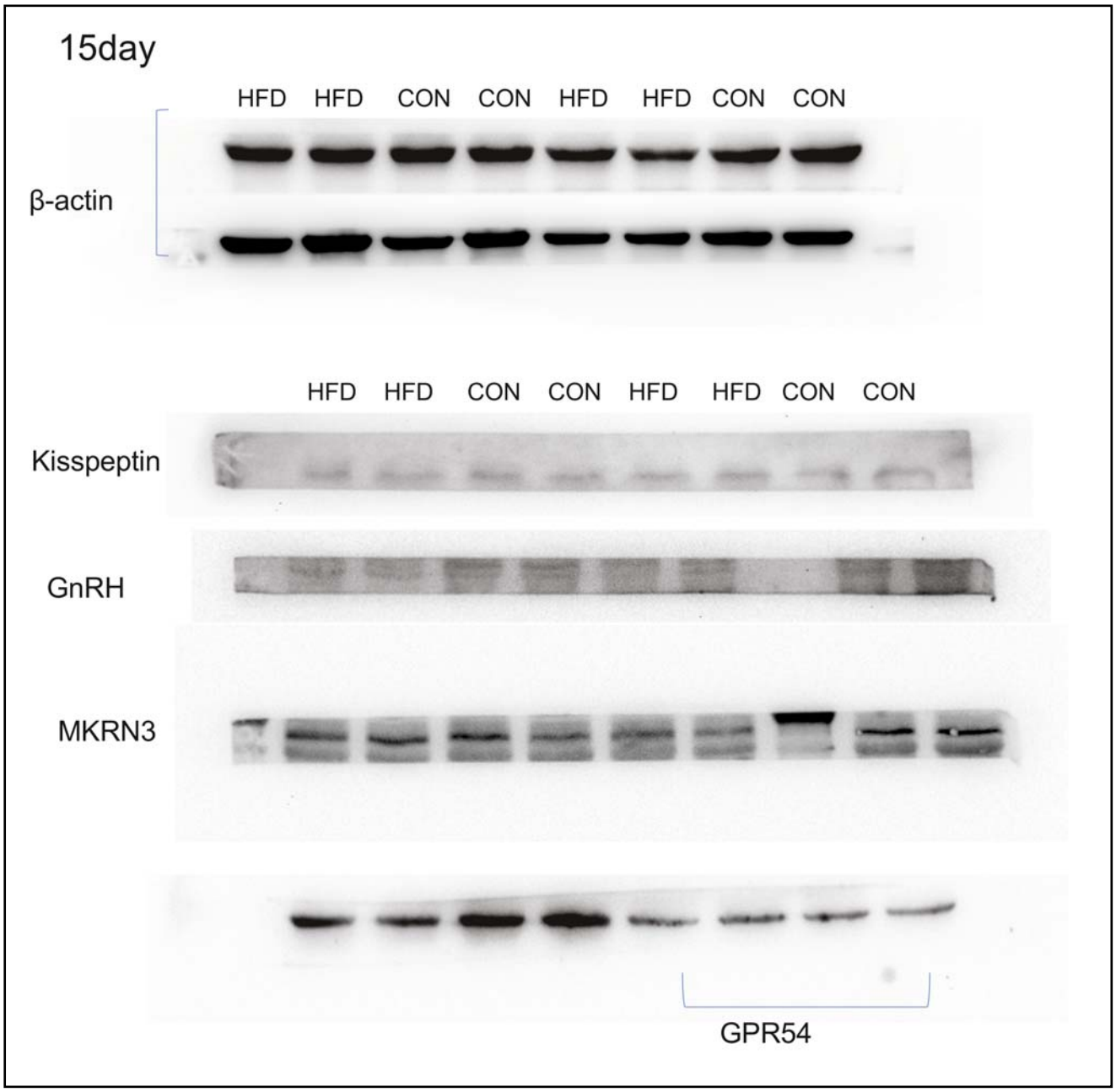

Supplementary Fig. 1.

SUPPLEMENTARY FIGURE 2 - FULL SIZE WESTERN BLOTS

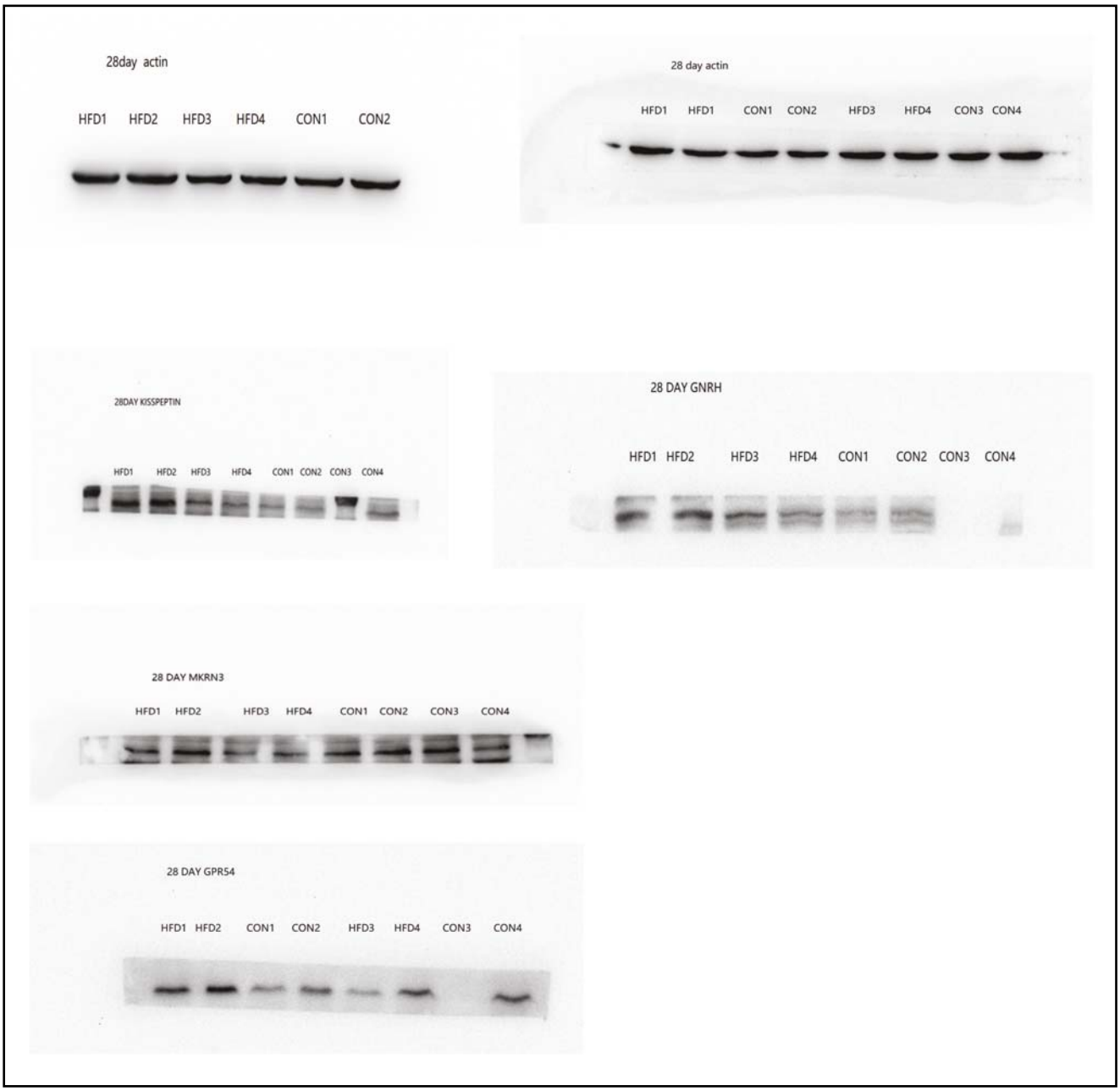

Supplementary Fig. 2.

SUPPLEMENTARY FIGURE 3 - FULL SIZE WESTERN BLOTS

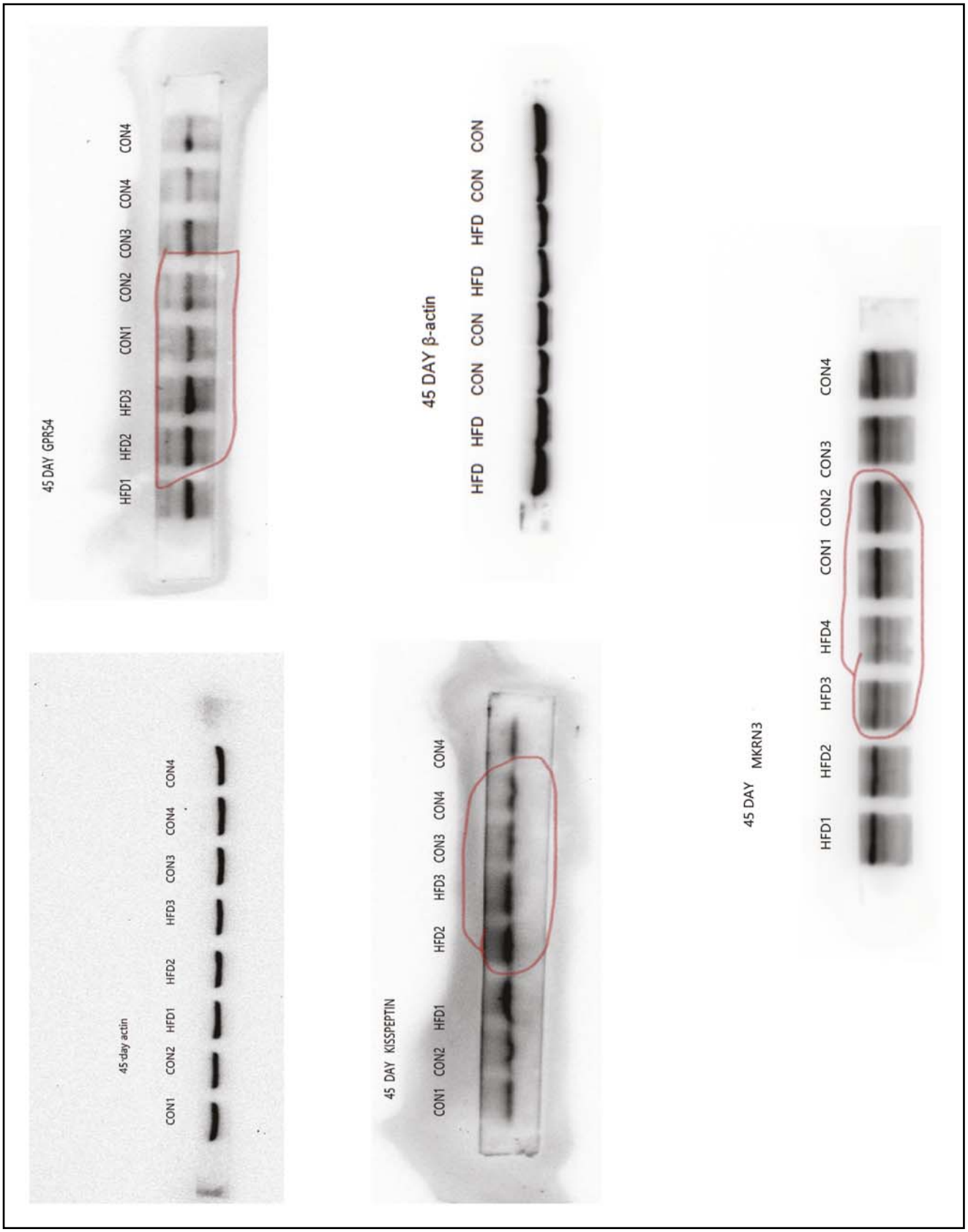

Supplementary Fig. 3.